Indian Journal of Chemistry
Vol. 61, June 2022, pp. 599-606

Synthesis of 9,9-dimethyl-12-(aryl)-8,9,10,12-tetrahydrobenzo[a]xanthene-11-ones by modified kaolinite nanoclay as an efficient and reusable heterogeneous catalyst *via* a green protocol

Abdolhamid Bamoniri[a], Reza Delqavi Khalifa lou[b] & Nahid Yaghmaeiyan*[a]

[a] Department of Organic Chemistry, Faculty of Chemistry, University of Kashan, Kashan, Iran

[b] Department of Chemistry, Ahar Branch, Islamic Azad University, Ahar, Iran

E-mail: nahidyaghma@yahoo.com

Received 17 August 2020; accepted (revised) 23 December 2021

9,9-Dimethyl-12-(aryl)-8,9,10,12-tetrahydrobenzo[a]xanthene-11-one derivatives have been prepared *via* three component reaction of various aromatic aldehydes, dimedone and 2-naphthol. This green methodology has been effectively catalyzed by sulfonyl- functionalized kaolinite nanoclay (nano-kaolin-SO_3H) as a recoverable solid catalyst. This type of solid acid which contains the properties of a Lewis acid (Al^{3+}cation) and a Brønsted acid (SO_3H group), has been characterized by ATR, TEM, FESEM, EDS, EDS mapping, XRD, TGA, BET and XRF techniques. Compared with conventional methods, this protocol has promising features for the reaction response such as simplicity in the experimental procedure, easier work-up, shorter reaction times and ease of separation of pure products with high yields.

Keywords: Nano-kaolin-SO_3H, xanthene,2-naphthol, dimedone, aromatic aldehyde, nanoclay, heterogeneous

Kaolinite with chemical composition $Al_2Si_2O_5(OH)_4$ is a raw, commercial, low-cost, easily available, non-corrosive and environmentally benign material formed by decomposition of feldspar. The primary structural unit of this structure is a layer composed of one alumina octahedral sheet condensed with one silicate tetrahedral sheet through oxygen atoms[1]. Its colour, gloss and hardness are ideal characteristics for the production of paper, cement, ceramics, bricks, adsorbent for pollutants, porcelain and catalysts[2-8]. However, despite economic advantages of kaolinite, it has inherent limitations such as porosity, impurities, low surface area and acidity which hindered their wide and sustained acceptability. So it seems necessary to modify the structure of kaolinite. Because of the naturally abundance of kaolinite, researchers are turning their attention to it again to prepare modified kaolinite as catalyst[9,10]. Modification of kaolinite structure have significant advantages such as its mechanical and chemical stability, improved surface area, and above all, high density of Lewis and Brønsted acid sites[11,12] with cation exchange capacity (CEC). Different modifiers have been used to increase catalytic activity of kaolinite. These methods including chemical activation[12], intercalation[13], mechanochemical[14,15], and thermal treatments[12,13]. Nano kaolin-SO_3H as a reusable and green heterogeneous nano-catalyst was prepared by the reaction of commercial kaolinite nanoclay with chlorosulfonic acid. The large pore size of this catalyst makes it a convenient bed for the conversion of bulky molecules. It could be an efficient solid acid catalyst for the promotion of many organic reactions.

Xanthene and its derivatives are pharmaceutically and biologically active compounds[16,17] which possess antiviral[18], anti-proliferative[19] and anti-inflammatory[20] activities. It's skeleton play a key role in polycyclic structures of some natural sources[21]. Xanthenes are also used extensively in the preparation of dyes[22] and laser technologies[23]. Moreover, xanthenes are used as sensitizers in photodynamic therapy for destroying the tumor cells[24] and pH-sensitive fluorescent materials for visualization of biomolecules[25]. More widespread synthetic approaches for preparation of tetrahydroxanthenones are the cyclocondensation of 2-naphthol, aromatic aldehydes and cyclic 1,3-dicarbonyl compounds under different conditions. More recently, various catalysts such as $NaHSO_4.SiO_2$[26], strontium triflate[27], indium (III) chloride or P_2O_5[28], dodecatungstophosphoric acid[29], iodine[30], HBF_4/SiO_2[31], sulfamic acid[32], cyanuric

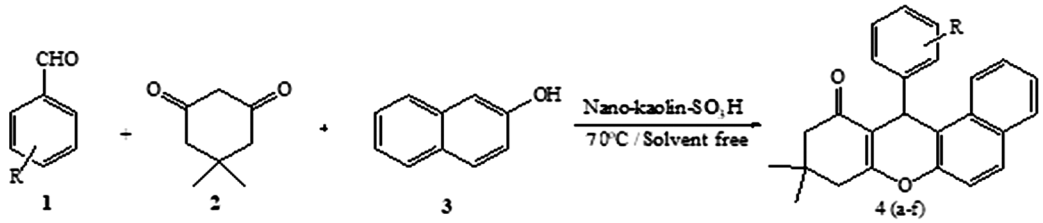

Scheme I — Synthesis of tetrahydroxanthenone derivatives using nano-kaolin-SO_3H in solvent free condition at 70°C

chloride[33], Cu/SiO_2[34], $H_4SiW_{12}O_{40}$[35], ruthenium chloride[36], Caro's acid–silica gel[37], camphor sulfonic acid[38]and nano-silica phosphoric acid[39] have been reported for the synthesis of tetrahydroxanthenones in different conditions such as solid state grinding, solid state heating, stirring in water and reflux. However, in spite of their potential utility, some of these methods have their own merits as well as demerits such as use of toxic and hazardous solvents, expensive catalyst and solvent, harsh reaction conditions, longer reaction time, requirement of huge amounts of catalyst, poor yields and difficulties in work-up procedure. Therefore, the development of a clean, simple and efficient procedure with high yielding and eco-friendly approach based on green methodology is still in demand. In this regard, herein a simple and efficient method for the one-pot synthesis of 12-aryl-8,9,10,12-tetrahydro-benzo[a]xanthen- 11-one derivatives in the presence of nano-kaolin-SO_3H is reported. During the course of our studies to avoid of using the toxic organic solvents and due to the advantages of multi-component reactions, we have designed an environmentally benign procedure for the one-pot synthesis of tetrahydroxanthenone derivatives using nano-kaolin-SO_3H as an efficient and reusable catalyst in solvent free conditions at 70°C (Scheme I).

Experimental Section

Chemicals such as dimedone, aromatic aldehyde derivatives, 2-naphthol, chlorosulfonic acid, kaolinite nanoclay, ethanol, methanol and peterolium ether were purchased from Fluka, Merck and Aldrich Chemical Co. ^{1}H NMR spectra were recorded on a Avance BRUKER (DRX-400MHz) in $CDCl_3$and DMSO-d_6 as the solvents. Thin layer chromatography (TLC) on commercial aluminium-backed plates of silica gel 60 F_{254} was used to monitor the progress of the reactions. Melting points were obtained with a micro melting point apparatus (Electrothermal, Mk3). IR spectra were determined on a Nicolet Magna series FT-IR 550 spectrometer using KBr pellets. Average size of nanoparticles was analyzed by TEM using a Zeiss EM900 with a LaB6 cathode and accelerating voltage of 200 kV. The morphology and size of nanoparticles have been characterized using KYKY-EM3200, 26 kV field emission scanning electron microscope (FESEM). Quantitative elemental information (EDS) of nanoparticles was measured by EDS instrument, Phenom pro X. XRD patterns were collected on a Philips Xpert MPD diffractometer equipped with a Cu Kα anode (λ=1.54 A˚) in the 2θ range from 10 to 80°. TGA curves were recorded using BAHR/STA503 at the range of 0-550°C. Specific surface area of the modified catalyst was measured by Micromeritics, Tristar II 3020 analyzer. Elemental composition was investigated by XRF BRUKER S4 EXPLORER.

General procedure for preparation of tetra-hydroxanthenones

A mixture of dimedone (1mmol), 2-naphthol (1mmol),aromatic aldehyde (1mmol) and optimized amount of nano-kaolin-SO_3H (0.02g) were added in a 50 mL round-bottomed flask. The mixture was stirred for110-173 minutes at 70°C under solvent free conditions. After completion of the reaction followed by TLC, the reaction mixture was cooled to room temperature and washed with hot ethanol for several times. The product was separated from the catalyst by filtration.Nano-kaolin-SO_3H reused for the next experiment and the solvent was evaporated. The solid product was recrystallized from petroleum ether/ethanol in 6:1 ratio to afford the pure product in high yield. The results of synthesis of tetrahydroxanthenones in the presence ofnano-kaolin-SO_3Hat 70°C under solvent free conditions are summarized in Table I.

One of the outstanding advantages for the solid acid catalysts are their reusability and stability which makes them valuable for commercial applications. Thus, after completion of the reaction for the synthesis of **4e**, the reaction mixture was washed with hot ethanol and the catalyst was separated by filtration. The recovered catalyst was washed with chloroform (3×10 mL) and dried at room temperature without further purification to use for the

Table I — One pot synthesis of tetrahydroxanthenones in the presence of nano-kaolin-SO_3H at 70°C under solvent free conditions

Entry	ArCHO	Product	Time (min)	Yeild (%)	m.p. (°C)		Ref
					Obtained	reported	
1	C_6H_5	**4a**	139	91	150-152	151-153	28
2	4-ClC_6H_4	**4b**	131	93	179-181	180-182	28
3	4-$(CH_3)C_6H_4$	**4c**	156	88	173-175	176-178	28
4	2- $NO_2C_6H_4$	**4d**	150	92	224-226	223-225	28
5	4-$NO_2C_6H_4$	**4e**	110	96 2nd run 95 3nd run 93 4nd run 89	179-181	178-180	28
6	3- $NO_2C_6H_4$	**4f**	118	93	167-169	168-170	28
7	4-OH C_6H_4	**4g**	167	85	221-223	223-225	28
8	4- $(CH_3O)C_6H_4$	**4h**	173	87	206-208	204-205	28
9	2-ClC_6H_4	**4i**	135	90	178-180	179-180	28
10	2,4- ClC_6H_3	**4j**	144	92	181-183	178-180	28

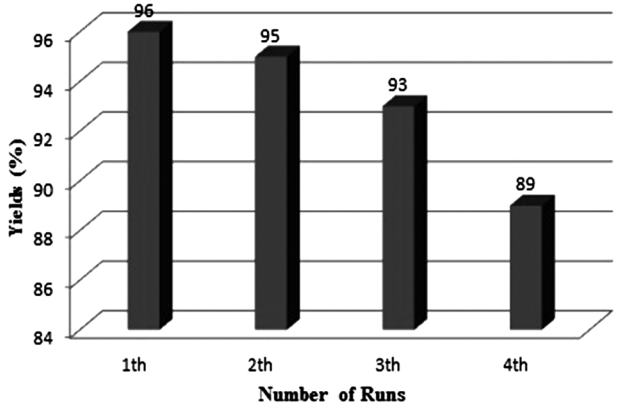

Figure 1 — Reusability diagram of nano-kaolin-SO_3H

next run in current reaction under equal condition. It was found that the catalyst could be reused for 3 times without any considerable loss of its activity (Figure 1).

Selected spectroscopic data

9,9-Dimethyl-12-(4-methylpheny)-8,9,10,12-tetrahydrobenzo[a]xanthene-11-one, 4c: White solid. 88% Yield. mp/°C: 173-175 (Lit. 176-178[28]). $\bar{\upsilon}_{max}$ (KBr)/cm^{-1}: 3015 (=C-H), 2958 (-C-H), 1667 (C=O), 1596-1417 (C=C), 1374 (CH_3, bending), 1300-1000 (C-O), 831 (=C-H bending OOP of para disubstituted phenyl ring). ^{1}H NMR (DMSO-d_6)/ppm: δ_H= 8.01 (1H, d, $^3J_{HH}$ = 7.6 Hz, Ar-H), 7.49 (2H, d, $^3J_{HH}$ = 8.4 Hz, Ar-H), 7.55-7.42 (3H, m, Ar-H), 7.15 (2H, d, $^3J_{HH}$ = 8.0 Hz, Ar-H), 6.96 (2H, d, $^3J_{HH}$ = 8.0 Hz, Ar-H), 5.50 (1H, s, CH), 2.68 (2H, d, $^2J_{HH}$ = 17.6 Hz, CH_2C=O), 2.56 (2H, d, $^2J_{HH}$ = 17.6 Hz, CH_2C=O), 2.32 (2H, d, $^2J_{HH}$ = 16.4 Hz, CH_2), 2.15 (2H, d, $^2J_{HH}$ = 16.4 Hz, CH_2), 2.12 (3H, s, CH_3), 1.05 (3H, s, CH_3), 0.88 (3H, s, CH_3).

9,9-Dimethyl-12-(4-hydroxypheny)-8,9,10,12-tetrahydrobenzo[a]xanthene-11-one, 4g: Pale yellow solid. 85% Yield. mp/°C: 221-223 (Lit. 223-225[28]). $\bar{\upsilon}_{max}$ (KBr)/cm^{-1}: 3309 (O-H), 3050 (=C-H), 2955 (-C-H), 1717 (C=O), 1642-1400 (C=C), 1366 (CH_3, bending), 1251 (Ar-O), 1300-1000 (C-O), 850 (=C-H bending OOP of para disubstituted phenyl ring). ^{1}H NMR (DMSO-d_6)/ppm: δ_H= 9.20 (1H, s, OH), 8.12 (1H, d, $^3J_{HH}$ = 9.2 Hz, Ar-H), 7.88 (2H, t, $^3J_{HH}$ = 9.2 Hz, Ar-H), 7.44-7.32 (3H, m, Ar-H), 7.26 (2H, d, $^3J_{HH}$ = 8.0 Hz, Ar-H), 6.65 (2H, d, $^3J_{HH}$ = 8.0 Hz, Ar-H), 5.63 (1H, s, CH), 2.70 (2H, d, $^2J_{HH}$ = 16.4 Hz, CH_2C=O), 2.61 (2H, d, $^2J_{HH}$ = 16.4 Hz, CH_2C=O), 2.32 (2H, d, $^2J_{HH}$ = 16.0 Hz, CH_2), 2.10 (2H, d, $^2J_{HH}$ = 16.0 Hz, CH_2), 1.05 (3H, s, CH_3), 0.88 (3H, s, CH_3).

9,9-Dimethyl-12-(4-methoxypheny)-8,9,10,12-tetrahydrobenzo[a]xanthene-11-one, 4h: White solid. 87% Yield. mp/°C: 206-208 (Lit. 204-205[28]). $\bar{\upsilon}_{max}$ (KBr)/cm^{-1}: 3015 (=C-H), 2955 (-C-H), 1648 (C=O), 1597-1462 (C=C), 1377 (CH_3, bending), 1300-1000 (C-O), 831 (=C-H bending OOP of para disubstituted phenyl ring). ^{1}H NMR (DMSO-d_6)/ppm: δ_H= 8.05 (1H, d, $^3J_{HH}$ = 7.6 Hz, Ar-H), 7.95 (2H, d, $^3J_{HH}$ = 8.4 Hz, Ar-H), 7.48-7.38 (3H, m, Ar-H), 7.15 (2H, d, $^3J_{HH}$ = 8.0 Hz, Ar-H), 6.72 (2H, d, $^3J_{HH}$ = 8.0 Hz, Ar-H), 5.50 (1H, s, CH), 3.61 (3H, s, OCH_3), 2.68 (2H, d, $^2J_{HH}$ = 17.6 Hz, CH_2C=O), 2.46 (2H, d, $^2J_{HH}$ = 17.6 Hz, CH_2C=O), 2.36 (2H, d, $^2J_{HH}$ = 16.4 Hz, CH_2), 2.15 (2H, d, $^2J_{HH}$ = 16.4 Hz, CH_2), 1.05 (3H, s, CH_3), 0.90 (3H, s, CH_3).

Results and Discussion

Preparation and characterization of nano-kaolin-SO_3H

For the preparation of nano-kaolin-SO_3H as an efficient and reusable catalyst,20 mL chlorosulfonic

acid was added drop-wise to a mixture of 5g kaolin nanoclayand25 mL chloroform in a ventilated cabinet. The resulting suspension was stirred for 15minutes at room temperature, filtered, washed with chloroform, and dried at room temperature.

The acidic capacity of prepared nano-kaolin-SO_3H was determined *via* titration of 0.05g of it with 12.16 mL NaOH 0.009 N. The result was shown 2.268 meq/g H^+. The acidity of the catalyst was compared with kaolinite. The pH of 0.05 g of commercial kaoliniteandnano-kaolin-SO_3H in 5 mL of distilled water was 6 and 3.4, respectively.

Figure 2 shows the FT-IR (ATR) spectra of kaolinite nanoclay and nano-kaolin-SO_3H. In FT-IR spectrum of kaolinite (Figure 2a), several bands at 3686, 3620, 1114, 990, 909, 791, 752 and 640 cm^{-1} were existed which correspond to inner Al-OH, outer Al-OH, unsymmetrical Si-O-Si, symmetrical Si-O-Si, Al-O-H bending and unsymmetrical/symmetrical Si-O-Si of quartz, respectively[40,41]. However, in the nano-kaolin-SO_3H spectrum (Figure 2b), in addition to above mentioned bands, a band at 1160 cm^{-1} and a very broad band at 2700-3400 cm^{-1} were appeared. The broad band at 1160 $cm^{1}$and a very broad band at 2700-3400 cm^{-1} verify the O=S=O and –SO-H vibrations on nano-kaolin-SO_3H, respectively.

The transition electron microscope (TEM) images of nanoparticleagglomerations of kaolinite nanoclay and nano-kaolin-SO_3H have been displayed in Figure 3a and Figure 3c in the scale of 40 and 20 nm, respectively. These images clearly show the amorphous surface morphology of the nanoparticles. A collection of small particles with nearly spherical shape and an average size distribution of 50 and 15 nm creates big amorphous and non-uniform particles in kaolinite nanoclay and nano-kaolin-SO_3H, respectively. Selected area diffraction patterns (SADPs) of kaolinite nanoclay and nano-kaolin-SO_3H verify the amorphous morphology of the catalysts and collections of a large number of crystals with different orientations. This patterns are composed of concentric rings in that individual reflections are seen within the rings (Figure 3b,d).

For the characterization of the surface morphology, the FESEM micrographs of kaolinite nanoclay and nano-kaolin-SO_3H were prepared (Figure 4a-d). Figure 4a shows that naked kaolinite nanoclay composed from amorphous aggregations of small and relatively uniform nanoparticles which have a nearly spherical shape. Average size distribution of these nanoparticles is47.76 nm. In addition of these particles, kaolinite nanoclay has a layered morphology consisting of broken plates. A selected surface area of Figure 4a is shown in Figure 4b which shows that the thickness of layers is about 80nm. The surface of layers is also covered with nanoparticles and aggregates. As can be seen from the inset of Figure 4c,d, the morphology of the nano-kaolin-SO_3H is quite similar to that of the parent nanoclay. The micrographs of nano-kaolin-SO_3H clearly show highly porous morphology of it. As can be seen from Figure 4d, the average diameter of holes in nano-kaolin-SO_3H is about 20 nm which makes it a convenient bed for the conversion of bulky molecules.

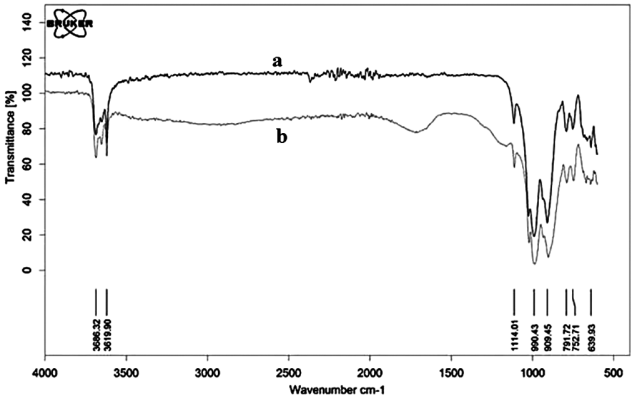

Figure 2 — FT-IR (ATR) spectra of (a) kaolinite nanoclay and (b) nano-kaolin–SO_3H

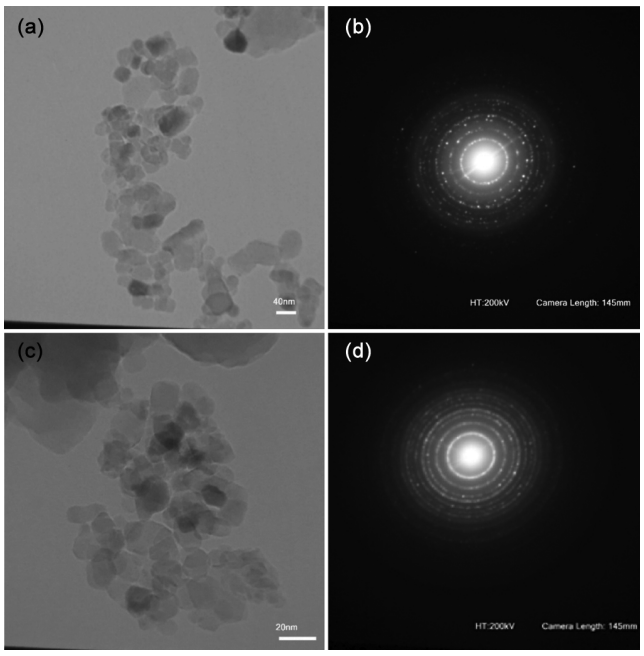

Figure 3 — (a)TEM image and (b) diffraction pattern of kaolinite nanoclay and (c) TEM image and (d) diffraction pattern of nano-kaolin-SO_3H

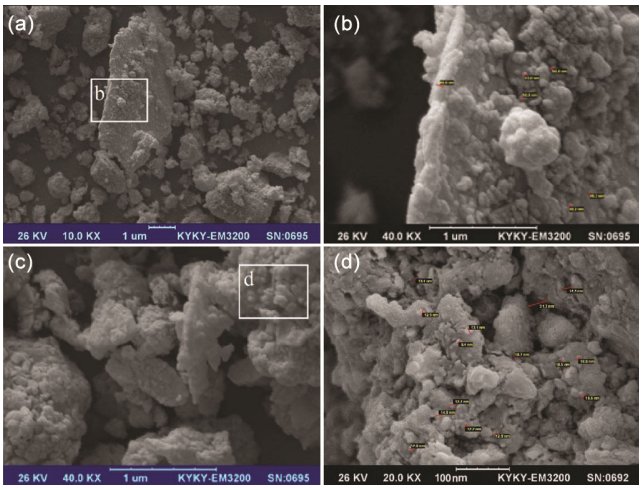

Figure 4 — FESEM of (a) kaolinite nanoclay, (b) a selected area of Figure 4a, (c) FESEM of nano-kaolin-SO_3H and (d) a selected area of Figure 4c

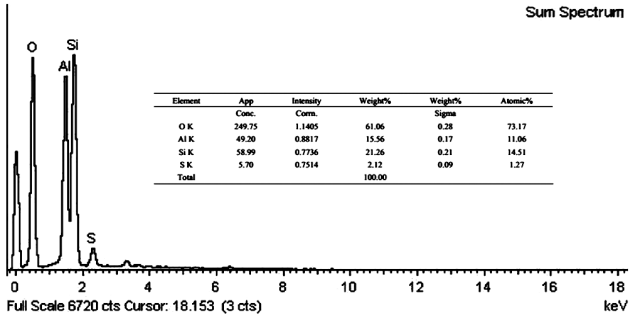

Figure 5 — Energy-dispersive X-ray spectroscopy (EDS) of nano-kaolin-SO_3H

The particle size of nano-kaolin-SO_3H was measured by FESEM and an average size distribution of 14.07 nm was obtained fornano-kaolin-SO_3H.

Energy-dispersive X-ray spectroscopy (EDS) of nano-kaolin-SO_3H measured by EDS instrument. According to this data, the weight percentage of O, Al, Si and S are 61.06, 15.56, 21.26 and 2.12, respectively (Figure 5)

The EDS mapping image of nano-kaolin-SO_3H are also demonstrated in Figure 6. The spatial distribution of elements O, Si, Al, and S is confirmed in this figure.

The X-ray diffraction (XRD) patterns of kaolinite nanoclay and nano-kaolin-SO_3H are shown in Figure 7a,b. As shown in Figure 7a and the results in peak list for kaolinite, peaks in 2θ values of 12.37, 20.45, 21.60, 23.20, 23.90, 24.99, 25.43, 27.33, 35.12, 36.73, 37.80, 38.17, 39.42, 40.1702, 41.32, 45.69, 46.89, 48.59, 49.64, 51.19, 55.52, 56.93, 58.19, 60.15, 62.58, 64,74, 65.44, 67.90, 68.99, 70.52, 72.39, 73.54,

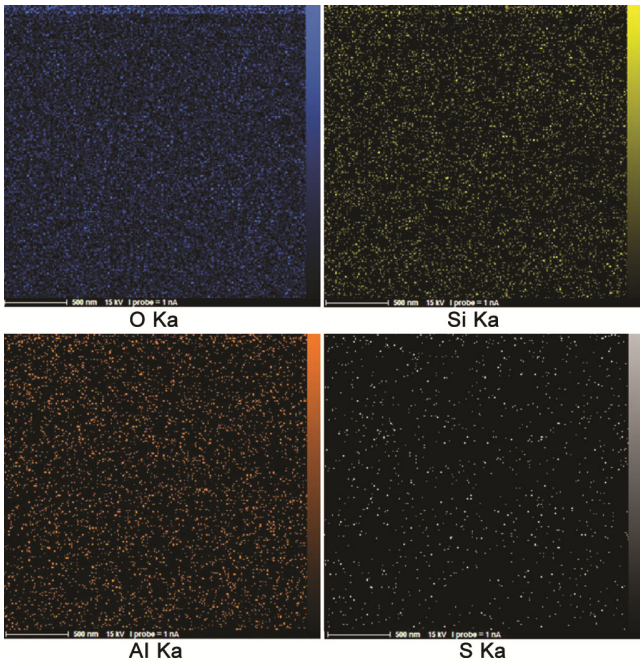

Figure 6 — The EDS mapping images of nano-kaolin-SO_3H and spatial distribution of elements O, Si, Al, and S

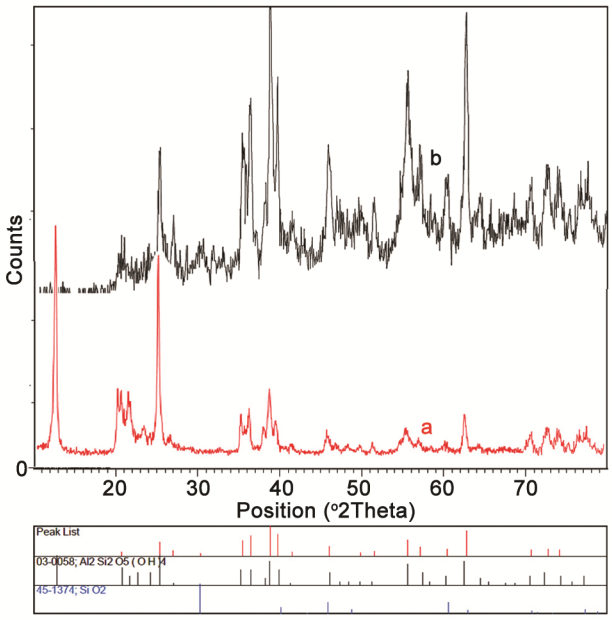

Figure 7 — X-ray diffraction (XRD) patterns of (a) kaolinite nanoclay and (b) nano-kaolin-SO_3H

75.90 and 76.13 verify the kaolinite structure. Incorporation of -SO_3H leads to some changes in the diffractogram of nano-kaolin-SO_3H (Figure 7b). In the diffractogram of kaolinite nanoclay in 2θ from 63 to 80, there were nine peaks (from 64,7473 to 76.1325) but in nano-kaolin-SO_3H there were only three peaks (at 70.60, 72.67 and 74.08). In nano-

kaolin-SO_3H, three peaks in 2θ from 21 to 24 (at 21.60, 23.20 and 23.90) disappeared. Other peaks in kaolinite and nano-kaolin-SO_3H diffractograms were in the same positions. The sharpness of peaks in the nano-kaolin-SO_3H diffractogram shows crystalline form for the catalyst. Using the Scherrer equation shows that the average size of particles is about 54.59 and 16.71 nm for kaolinite nanoclay and nano-kaolin-SO_3H, respectively.

TGA-DTG curves of starting kaolinite displays a strong peak at 517°C, which is due to dehydroxylation of kaolinite within the 450-600°C temperature range resulting in a weight loss of 15.34% and formation of metakaolinite. The peak on the TG-DTG curve at approximately 980°C is an evidence of the metakaolinite structure breakdown and the formation of mullite. Thermal gravimetric analysis (TGA-DTG) pattern of kaolin-SO_3H nanoparticles was detected from 20 to 510°C (Figure 8). The catalyst is stable until 50°C and only 4.16% of its weight was reduced in 50°C. Three endothermic processes were accrued between 50-190°C due to decomposition of –SO_3H group and elimination of SO_2 and H_2O from catalyst. Between 190-330°C, its weight is nearly constant and only 3.37% of mass was reduced. Two processes between 330-460°C and 460-510°C caused mass changed equal to 3.77% and 14.4%, respectively due to dehydroxylation of kaolinite.

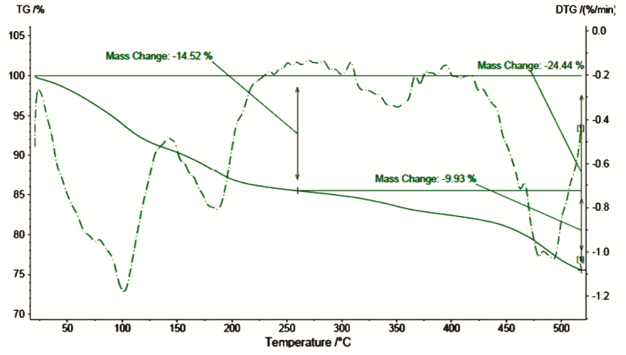

Figure 8 — Thermal gravimetric analysis (TGA-DTG) pattern of nano-kaolin-SO_3H

Specific surface area of catalyst was measured by BET theory. The single point surface area at P/Po= 0.983 is 7.59 m²/g, while the mean pore diameter is 20.601 nm and the total pore volume is 3.909 cm^3g^{-1}. The N_2 adsorption isotherm of catalyst is shown in Figure 9.

The results of X-ray fluorescence of nano-kaolin-SO_3H are shown the presence of 43% SiO_2, 30.5% Al_2O_3, 15.9% SO_3 and 8.2% CO_2 in the its composition. (Table II). Presence of 15.9% SO_3 in the composition of catalyst verify to structure of nano-kaolin-SO_3H.

Optimization of reaction conditions

To find the optimum conditions (solvent, amount of catalyst and temperature) for the synthesis of tetrahydroxanthenones in the presence of nano-kaolin-SO_3H, we have synthesized tetrahydroxanthenones in the presence of nano-kaolin-SO_3H under various conditions (Table III). Reactions at different conditions revealed that the best conditionswere presented at 70 °C in solvent free conditions. The reusability of the nano-kaolin-SO_3H was also examined for three times. (Entries 16-18). The catalyst was reusable, although a gradual decline in activity was observed. The reaction was done in a ratio of aldehyde (mmol): 2-naphthol (mmol): dimedone (mmol): nano-kaolin-SO_3H (g) equal to 1:1:1:0.02. In the presence of more nano-catalyst, it is possible to form side products

Mechanism of the reaction

A possible mechanism for the one-pot, three component condensation reaction of aromatic

Table II — The results of X-ray fluorescence of nano-kaolin-SO_3H

Element	SiO_2	Al_2O_3	SO_3	CO_2
Percent%	43	30.5	15.9	8.2

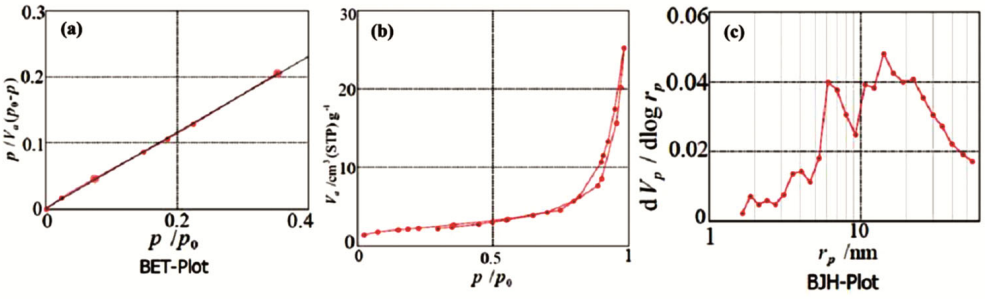

Figure 9 — (a) BET (Brunauer–Emmett–Teller), (b) adsorptiondesorption isotherm and (c) BJH (Barrett-Joyner-Halenda) plots of nano-kaolin-SO_3H

Table III — Optimization of reaction conditions (solvent, amount of catalyst and temperature) for preparation of **4e**

Entry	Solvent	Catalyst (g)	Temperature (°C)	Time (min)	Yield (%)
1	H_2O	–	RT	360	0
2	H_2O	0.005	RT	360	10
3	EtOH	0.005	RT	360	trace
4	MeOH	0.005	RT	360	trace
5	–	0.005	RT	360	13
6	–	0.005	20	360	17
7	–	0.005	40	360	25
8	–	0.005	50	360	33
9	–	0.005	60	360	39
10	–	0.005	70	360	44
11	–	0.005	80	360	44
12	–	0.010	70	300	92
13	–	0.015	70	150	92
14	–	0.020	70	110	96
15	–	0.02	70	110	96
16 (2^{nd} run)	–	0.02	70	110	95
17 (3^{rd} run)	–	0.02	70	110	93
18 (4^{th} run)	–	0.02	70	110	89

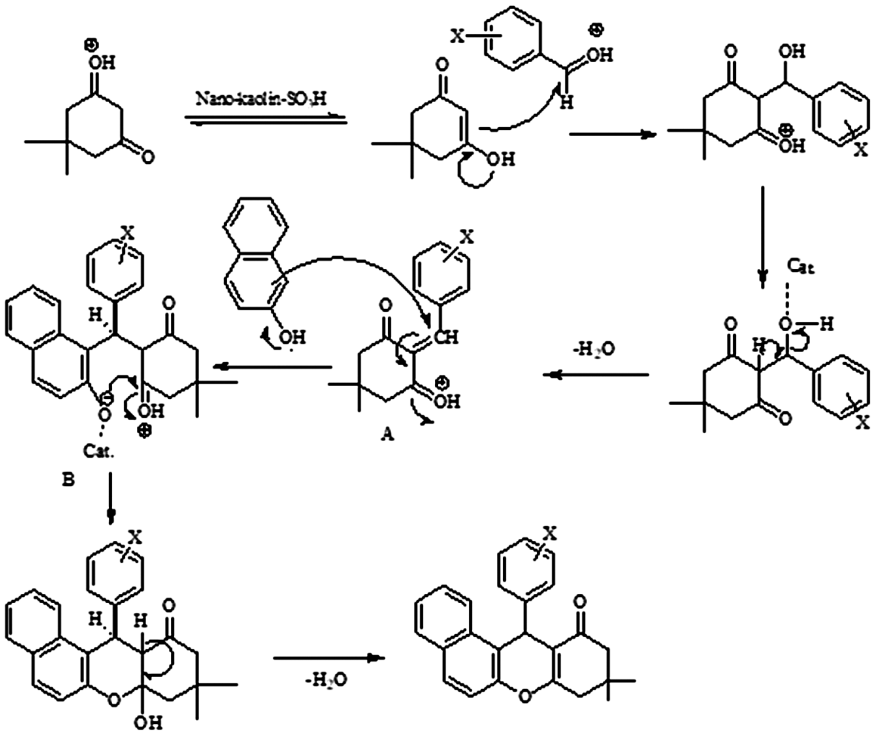

Scheme II — Proposed mechanism for one-pot synthesis of tetrahydroxanthenones in the presence of nano-kaolin-SO_3H

aldehyde, 2-naohthol and dimedone, in the presence of nano-kaolin-SO_3H is shown in Scheme II. According to the suggested mechanism, at first, nano-kaolin-SO_3H activates the carbonyl groups of dimedone and aldehyde and then the nucleophilic attack occurs at the activated carbonyl of aldehyde to result intermediate **A**. The catalyst then activate the carbonyl group of dimedone in the intermediate **A** and the C_α of 2-naphthol. This time the nucleophilic attack occurs from C_α of 2-naphthol at the $C_\beta$of α, β-unsaturated system of intermediate **A**to produce intermediate **B**. Then, cyclization of intermediate **B** is done for the synthesis of tetrahydroxanthenone.

Conclusion

In conclusion, we have successfully developed an efficient, atom-economical, environment friendly and simple protocol for the synthesis of tetrahy-

droxanthenones. Use of a catalytic amount of nano-kaolin-SO_3H, simple manipulation, short reaction time and mild reaction conditions contribute to the significant features of this methodology. The nano-catalyst is efficient, non-hazardous, inexpensive and heterogeneous can be easily recovered from the reaction mixture *via* simple filtration and reused several times.

Acknowledgement

The authors are grateful to University of Kashan for supporting this work by Grant No. 159189/30.

Refrences

1 Deer W A, Howie R A & Zussman J, *An introduction to the rock-forming minerals*, second ed, (Longman Scientific & Technical, London), 1992.
2 Murray H H, *Appl Clay Sci,* 17 (2000) 207.
3 Cravero F, Gonzalez I, Galan E & Dominguez E, *Appl Clay Sci*, 12 (1997) 27.
4 Prasad M S, Reid K J & Murray H H, *Appl Clay Sci*, 6 (1991) 87.
5 Murray H H, *Appl Clay Sci*, 5 (1991) 379.
6 Burst J F, *Appl Clay Sci*, 5 (1991) 421.
7 Largo O R, de la Villa R V, Isabel de Rojas M I S & Frías M, *J Am Ceram Soc*, 92 (2009) 2443.
8 Murray H H & Kogel J E, *Appl Clay Sci*, 29 (2005) 199.
9 Panda A K & Singh R K, *J Fuel Chem Technol*, 39 (2011) 198.
10 Vaccari A, *Appl Clay Sci*, 14 (1999) 161.
11 Bhattacharyya K G & Gupta S S, *Desalination,* 272 (2011) 66.
12 do Nascimento L A S, Tito L M Z, Angélica R S, da Costa C E F, Zamian J R & Filho G N R, *Appl Catal B Environ*,101 (2011) 495.
13 Makó É, Senkár Z, Kristóf J & Vágvölgyi V, *J Colloid Interface Sci*, 294 (2006) 362.
14 Vágvölgyi V, Kovács J, Horváth E, Kristóf J & Makó É, *J Colloid Interface Sci*, 317 (2008) 523.
15 Kinjo J, Uemura H, Nohara T, Yamashita M, Marubayashi N & Yoshihira K, *Tetrahedron Lett*, 36 (1995) 5599.
16 El-Brashy A M, Metwally M E & El-Sepai F A, *Farmaco*, 59 (2004) 809.
17 Horvátha E, Frost R L, Makóc É, Kristóf J & Cseh T, *Thermochim Acta*, 404 (2003) 227.
18 Chibale K, Visser M, Schalkwyk D V, Smith P J, Saravanamuthu A & Fairlamb A H, *Tetrahedron*, 59 (2003) 2289.
19 Poupelin J P, Saint-Ruf G, Foussard-Blanpin O, Narcisse G, Uchida-Ernouf G & Lacroix R, *Eur J Med Chem,* 13 (1978) 67.
20 Kumar A, Sharma S, Maurya R A & Sarkar J, *J Comb Chem*, 12 (2010) 20.
21 Hideo T & Teruomi J, *Jpn Patent No.* 56005480, Jan 20, 1981.
22 Bhowmik B B & Ganguly P, *Spectrochim Acta A,* 61 (2005) 1997.
23 Ahmad M, King T A, Ko D K, Cha B H & Lee J, *J Phys D Appl Phys*, 35 (2002) 1473.
24 Ion R M, Planner A, Wiktorowicz K & Frackowiak D, *Acta Biochim Pol*, 45 (1998) 833.
25 Knight C G & Stephens T, *Biochem J*, 258 (1989) 683.
26 Das B, Laxminarayana K, Krishnaiah M & Srinivas Y, *Synlett*, (2007) 3107
27 Li J, Tang W, Lu L & Su W, *Tetrahedron Lett*, 49 (2008) 7117.
28 Nandi G C, Samai S, Kumar R & Singh M S, *Tetrahedron*, 65 (2009) 7129.
29 Wang H J, Ren X Q, Zhang Y Y & Zhang Z H, *J Braz Chem Soc*, 20 (2009) 1939.
30 Wang R Z, Zhang L F & Cui Z S, *Synth Commun*, 39 (2009) 2101.
31 Zhang Z H, Wang H J, Ren X Q & Zhang Y Y, *Monatsh Chem*, 140 (2009) Article 1481.
32 Heravi M M, Alinejhad H, Bakhtiari K & Oskooie H A, *Mol Divers*, 14 (2010) 621.
33 Zhang Z H, Zhang P, Yang S H, Wang H J & Deng J, *J Chem Sci*, 122 (2010) 427.
34 Oskooie H A, Heravi M M, Karimi N & Kohansal G, *Synth Commun*, 41 (2011) 2763.
35 Hassankhani A, Mosaddegh E &Ebrahimipour S Y, *E-J Chem*, 9 (2012) 786.
36 Tabatabaeian K, Khorshidi A, Mamaghani M, Dadashi A & Jalali M K, *Canadian J Chem*, 89 (2011) 623.
37 Karimi N, Oskooie H A, Heravi M M & Tahershamsi L, *Synth Commun*, 41 (2010) 307.
38 Shinde P V, Shingate B B & Shingare M S, *Lett Org Chem*, 8 (2011) 568.
39 Bamoniri A, Mirjalili B F & Nazemian S, *J Nanostruct*, 2 (2013) 433.
40 Diko M, Ekosse G & Ogola J, *Acta Geodyn Geomater*, 13 (2016) 149.
41 Saikia B J & Parthasarathy G, *J Mod Phys*, 1 (2010) 206.